Regular paper

Synergistic effect of Dactolisib/Lys05 combination on autophagy in A549 cells

Mohammad M. Abdelwahab[1], Hesham Saeed[1]✉, Nefertiti El-Nikhely[1] and Hisham A. Nematalla[2]

[1]Department of Biotechnology, Institute of Graduate Studies and Research, Alexandria University, Alexandria, Egypt; [2]Department of Pharmacology and Toxicology, Faculty of Pharmacy, Damanhour University, Damanhour, Egypt

Effective therapeutic strategies are urgently required to enhance the prognosis of patients suffering from KRAS mutations. Owing to the undruggable nature of KRAS, targeting downstream signaling pathways, namely PI3K/AKT/mTOR, shows antiproliferative and apoptotic effects. Unfortunately, targeting this pathway upregulates autophagy, contributing to reduced drug efficacy. Therefore, it was reasonable to use a combination of kinase inhibitors and autophagy inhibitors to achieve a higher therapeutic benefit. The impact of Dactolisib, a dual PI3K/mTOR inhibitor, and Lys05, a dimeric chloroquine, was tested on the survival of breast cancer MCF-7 and lung cancer A549 cells. The dose selection for the optimal effect of the Dactolisib/Lys05 combination was determined using CompuSyn software. This combinatorial effect was evaluated using various methodologies, such as expression profile analysis for autophagic, proliferative, and apoptotic markers. These effects were corroborated by ELISA, Western blot, and flow cytometry using the Annexin V-FITC apoptosis detection kit. A549 cells treated in a 2:1 ratio of Lys05 and Dactolisib demonstrated a synergistic effect on cell death, proliferation, and apoptotic gene markers, in addition to its effect on autophagic gene and protein markers, showing an enhanced effect compared to monotherapy. Therefore, the PI3K/AKT kinase inhibitor/autophagy inhibitor combination establishes higher therapeutic benefits on A549 cells compared to kinase inhibitor monotherapy.

Keywords: KRAS, autophagy, PI3K/Akt/mTOR, NSCLC, Dactolisib, Lys05

INTRODUCTION

Epidemiologically, lung cancer represents the leading cause of cancer-related deaths among both men and women (Barta *et al.*, 2019; Sun *et al.*, 2021). Our increasing understanding of cancer biology has revealed numerous causes for therapeutic failures (Rizzo, 2008). Research on signaling pathways has uncovered a complex network of cross-regulatory interactions, connecting receptors, enzymes, transducing systems, and transcription factors that regulate cell fate (Sever & Brugge, 2015).

Resistance to apoptosis, continuous proliferation, evasion from cell cycle suppressors, angiogenesis, invasion, and metastasis are the five features that characterize carcinoma (Hanahan & Weinberg, 2011). Autophagy, a further level of adaptation, is known to increase under conditions of cellular stress, particularly in cancer (Haider *et al.*, 2020; White & DiPaola, 2009).

Currently, non-small cell lung cancer (NSCLC) accounts for up to 85% of all lung cancers (El Osta *et al.*, 2019). Kirsten Rat Sarcoma Viral Oncogene Homolog (KRAS) is a gene that codes for a protein involved in cell signaling pathways. It is a well-known oncogene, meaning that mutations in the KRAS gene can contribute to the development of cancer. These mutations result in constant activation of the KRAS protein, leading to abnormal cell growth and division. KRAS mutation is among the most predominant mutations in NSCLC and shows little variation between early-stage and metastatic NSCLC (Ghimessy *et al.*, 2020; Lohinai *et al.*, 2017). The undruggable nature of KRAS, attributed to the inability to develop direct inhibitors that can effectively compete with its high affinity for GTP, and the lack of selectivity with wild-type RAS resulting in toxicity, has hindered the design of selective inhibitors targeting mutant KRAS (Chen *et al.*, 2020; Luo *et al.*, 2022). Inhibition of posttranslational modifications by farnesyltransferase inhibitors has also demonstrated minimal clinical activity (Adjei *et al.*, 2003; Heymach *et al.*, 2004).

A promising approach now is to target KRAS downstream signaling pathways, particularly PI3K/AKT/mTOR, as evidence suggests their upregulation in lung cancer, promoting cell survival, growth, proliferation, and migration (Huang *et al.*, 2021). The PI3K/Akt/mTOR pathway also plays a role in tumors with other activating mutations (Yu *et al.*, 2021), and increased PI3K or Akt activity regulates mTOR activity in lung cancer (Liang *et al.*, 2019). Treatment of NSCLC cells with mTOR inhibitors has been reported to significantly decrease cancer cell proliferation (Huang *et al.*, 2021). This signaling pathway plays a crucial role in the occurrence and progression of tumors by regulating autophagy and apoptosis of tumor cells (Lee *et al.*, 2021; Zou *et al.*, 2020).

Unfortunately, targeting the PI3K/Akt/mTOR pathway with various kinase inhibitors results in the upregulation of autophagy (Y. Liu *et al.*, 2021; Zhao *et al.*,

2015). Autophagy, as a cellular process in cancer, can both suppress and promote tumor growth, depending on the tissue and timing (Hanahan & Weinberg, 2011; Lim *et al.*, 2021). Furthermore, autophagy addiction characterizes KRAS-driven cancers, including NSCLC, as it replenishes mitochondria substrates required for acetyl-CoA synthesis (Eng *et al.*, 2016; White, 2012).

Given that the inhibition of the PI3K/Akt/mTOR pathway leads to the upregulation of autophagy, it was reasonable to consider a combination of kinase inhibitors and autophagy inhibitors to achieve a higher therapeutic benefit.

MATERIALS AND METHODS

Cell viability assay

Cancer cells MCF-7 and A549 were plated in 96-well plates at a density of 7000 cells/well in 100 µl of DMEM high glucose medium (4.5 g/L) supplemented with only 1% FBS overnight and 1% penicillin/streptomycin at 37°C and 5% CO_2. After serum starvation, cells were treated with Dactolisib (LC Laboratories, USA), and Lys05 (Sigma-Aldrich, China) at different concentrations for 48 h. For cytotoxicity assay using 3-(4,5-Dimethyl-2-thiazolyl)-2,5-diphenyl- 2H-tetrazolium bromide (MTT), MTT (5 mg/mL in 1×PBS) was added to the cells and incubated for 3 h at 37°C in 5% CO_2. A volume of 100 µL of DMSO was added to the cells to solubilize the formed formazan crystals with shaking. Finally, the absorbance was measured at 490 nm and the percentage of cell viability was calculated compared to the control (Kumar *et al.*, 2018).

Identification of synergism and antagonism in drug combination

Drug concentrations used in combination studies were selected from the dose–response data for individual agents in 1% FBS starved A549 cells. Fraction affected (Fa) values were calculated as the percentage inhibition of cell viability, relative to control, as described by Chou (Chou, 2006). Synergism, additivity, or antagonism of drug combinations was identified using the Chou Talalay Combination Index (CI) method (Chou, 2006) and CompuSyn software (http://www.combosyn.com) based mainly on the following equation:

$$CI = (D)_1/(D_x)_1 + (D)_2/(D_x)_2$$

where $(D)_1$ and $(D)_2$ represent the concentrations of Drug 1 and Drug 2 in the combination that produce a Fa value of x. $(D_x)_1$ and $(D_x)_2$ represent the concentrations of Drug 1 and Drug 2 that produce the same effect (x) when applied as single agents. CI values <1, =1, and >1 indicate synergism, additivity, and antagonism, respectively.

Protein determination and analysis by Sodium dodecyl sulphate polyacrylamide gel electrophoresis (SDS-PAGE) and western blotting

Protein concentration was determined according to Bradford using bovine serum albumin as a standard (Bradford, 1976). The total protein extract (50 µg) was mixed with a 5× sample application buffer, boiled for 5 min, and resolved on 14% SDS-PAGE. LC3B was detected through western blotting using anti-LC3B monoclonal antibody (Molecular weight 17.5 KDa) (Cell signaling, USA) at a dilution of 1:1000. The sec-ondary antibody used was goat anti-mouse IgG labeled with horse radish peroxidase (Invitrogen, USA) at a 1:1000 dilution. The nitrocellulose membrane was developed using enhanced chemiluminescence (ECL, Sigma-Aldrich, China)(Liu *et al.*, 2014). Beta-actin (ACTB) (Molecular weight 42 KDa) was used as a loading control.

Apoptosis detection by flow cytometry

Apoptosis was analyzed using Annexin V-FITC apoptosis detection kit (Miltenyi Biotec.). A549 cells were treated with Lys05, Dactolisib and the synergistic combination dose for 48 h. After incubation, cells were harvested by centrifugation, re-suspended in binding buffer, and incubated with fluorescein isothiocyanate (FITC)-labeled with Annexin V for 15 min in the dark at room temperature. Cells were then washed twice with 1×PBS and resuspended in binding buffer, propidium iodide was added, and cells were incubated for 15 min in the dark at room temperature (Lakshmanan & Batra, 2013). The stained cells were analyzed using BD FACS flow cytometer (BD Biosciences) at the flow cytometry service core facility at the Center of Excellence for Research in Regenerative Medicine and its Applications (CERRMA), Faculty of Medicine, Alexandria University.

Quantitative RT-PCR

Total RNA was isolated and purified from the treated and untreated A549 cells using TRIzol reagent (Qiagen, Germany) following the manufacturer's protocol (Rio *et al.*, 2010). The concentration and purity of RNA were determined using Nanodrop. One microgram of the total RNA was reverse transcribed into the first strand cDNA using a High-Capacity cDNA Reverse Transcription Kit (Applied Biosystems) using random hexamer primers according to the manufacturer's instructions. Quantitative real-time PCR was carried out in triplicates using Maxima SYBR Green qPCR Master Mix (ThermoFisher). Primers used were as follows: *HPRT* forward primer, 5'-TGACACTGGCAAAACAAT-3'; reverse, 5'-GGTCCTTTTCACCAGCAA-3'; *LC3A* forward primer, 5'-GGATTTTGAGGAGGGGACTC-3'; reverse, 5'-CATCTGCAAAACTGAGACAGTG-3'; *ATG4B* forward primer, 5'-GCAAGTCAAAAAGCT-GTCTCT-3'; reverse, 5'-CAGTCGCTCTACATCA-GAAGAA-3'; *LC3B* forward primer, 5'-CGAGA-GCAGCATCCAACCAA-3'; reverse, 5'-GAGCTGTAA-GCGCCTTCTAA-3'; *KI67* forward primer, 5'-GAG-GTGTGCAGAAAATCCAAA-3'; reverse, 5'-CTGTCC-CTATGACTTCTGGTTGT-3'; *CASP3* forward primer, 5'-TTTTTCAGAGGGGATCGTTG-3'; reverse, 5'-CG-GCCTCCACTGGTATTTTA-3'. Primers were added to the reaction mixture at a final concentration of 250 nM. The reaction was prepared in a final volume of 20 µL by mixing 5 µL of each cDNA sample (diluted 1:5), 12.5 µL of SYBR Green, 0.5 µL of each primer, and the final volume was adjusted through the addition of RNase/DNase free water. The reaction conditions used were as follows: 5 min at 95°C for 1 cycle followed by 40 cycles of 15 s at 95°C, 30 s at 58°C, and 30 s at 72°C. The specificity of each primer pair was verified by the presence of a single melting curve peak. Results were analyzed for the relative expression of mRNA normalized against hypoxanthine guanine phosphoribosyl transferase (HPRT) as a housekeeping gene. Finally, the results were analyzed, and expressed as fold change(Rao *et al.*, n.d.).
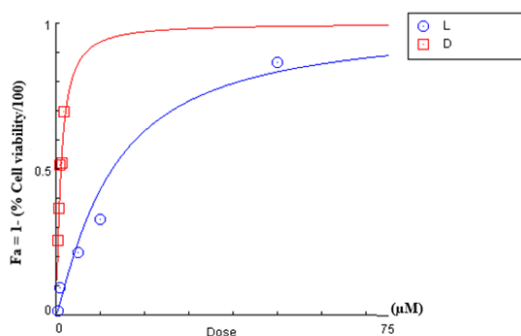
Figure 1. MTT cytotoxicity assay of Lys05 (L) and Dactolisib (D) on MCF-7.
Cells were treated with different concentrations of Lys05 and Dactoilisb for 48h. Data were normalized and IC50 values were 12.6 µM and 1.1 µM (n=5). The fraction affected "Fa" was calculated as 1 – (% Cell viability/100)

Figure 2. MTT cytotoxicity assay of Lys05 (L) and Dactolisib (D) on A549 cells.
A549 cells were treated with different concentrations of Lys05 and Dactolisib for 48h. Data were normalized and IC50 values on A549 for Lys05 was 11.8 µM and for dactolisib was 0.375 µM (n=5). The fraction affected (Fa) was calculated as 1 – (% Cell viability/100)

ELISA assay

Coated 96-well strip plate has been pre-coated with target-specific capture antibody LC3A (LifeSpan Bioscience, Inc.), LC3B (LifeSpan Bioscience, Inc.) and P62/SQSTM1 (MyBioSource, Inc.). A volume of 100 µL of the samples was added to the wells and incubated for 2 hours at 37°C. The liquid was aspirated and 100 µl of Biotin-labeled antibody working solution was added and incubated for 1 hour at 37°C. The liquid was aspirated then the wells were washed 3 times with wash buffer. The HRP-Streptavidin Conjugate working solution was added and incubated for 60 minutes at 37°C. The liquid was aspirated, and wells were washed 5 times with a wash buffer. The reaction was visualized by the addition of 90 µl of TMB Substrate solution and incubated for 15–30 minutes at 37°C. The reaction was stopped with 50 µl of sulfuric acid stop solution (1N H_2SO_4) to complete the color development reaction and then the ELISA plates were measured at a wavelength of 450 nm using a micro-plate Spectrophotometer.
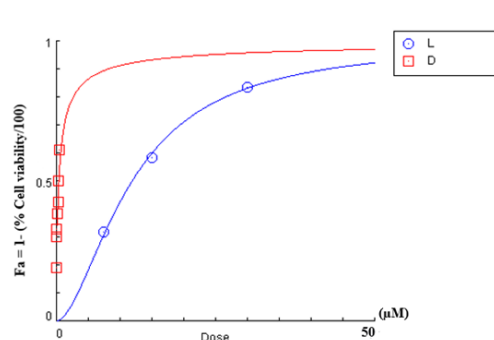
Statistical analysis

Data were presented as mean ± standard deviation and were evaluated by a univariate analysis of variance (ANOVA) Tukey's multiple comparisons test at $p<0.05$ using GraphPad Prism version 7.00, GraphPad, Software, San Diego California, USA. The IC_{50} values and Combination analysis were conducted as described by Chou using CompuSyn software (http:// www. combo syn. com).

RESULTS

The effect of the individual administration of dactolisib and Lys05 on MCF-7 and A549 cells

To evaluate the cell growth inhibitory effect of Dactolisib and Lys05 individually, the 3-(4,5-dimethylthiazol-2-yl)-2,5-diphenyltetrazolium bromide (MTT) assay was performed. The impact of both drugs on the survival of MCF-7 and A549 cells was examined to determine the IC50 values using GraphPad Prism version 7.0 and CompuSyn software version 1.

Increasing concentrations of Dactolisib and Lys05, as well as a clear culture media (control), were administered to MCF-7 and A549 cells. Figure 1 illustrates the dose-dependent reduction in cell viability caused by the individual administration of Dactolisib in MCF-7 cells compared to the control (untreated cells). The cytotoxic effect of Dactolisib was observed at a concentration of 1.1 µM (n=5) in MCF-7 cells.

Similarly, Fig. 2 shows the dose-dependent reduction in cell viability caused by the individual administration of Lys05 in A549 cells compared to the control. The cytotoxic effect of Lys05 was observed at a concentration of 0.375 µM (n=5) in A549 cells.

In summary, the individual administration of Dactolisib and Lys05 resulted in a dose-dependent reduction in cell viability in MCF-7 and A549 cells, respectively. Dactolisib exhibited cytotoxic effects at concentrations of 1.1 µM (n=5) in MCF-7 cells, while Lys05 showed cytotoxic effects at concentrations of 0.375 µM (n=5) in A549 cells.

A synergistic effect results from dactolisib/Lys05 combination on A549 cells

To investigate the combined cytotoxic effect of Dactolisib and Lys05, starved A549 cells were exposed to various combination ratios. The IC50 value of the 2:1 ratio (2L/1D) (0.05 µM Dactolisib + 3.19 µM Lys05)
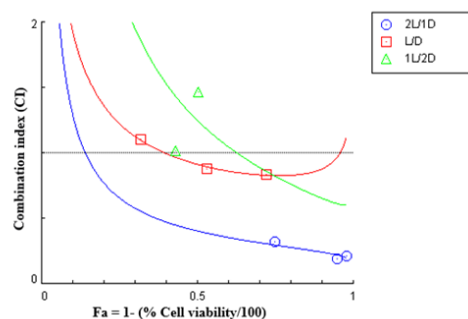
Figure 3. Combination index plot.

was determined, and it showed a significant effect below the additive line, indicating a synergistic effect. The combination index (CI) for this ratio was calculated as 0.4.

This finding suggests that the combination of Dactolisib and Lys05 at the specified ratio has a stronger cytotoxic effect on A549 cells compared to what would be expected if the effects of the two drugs were merely
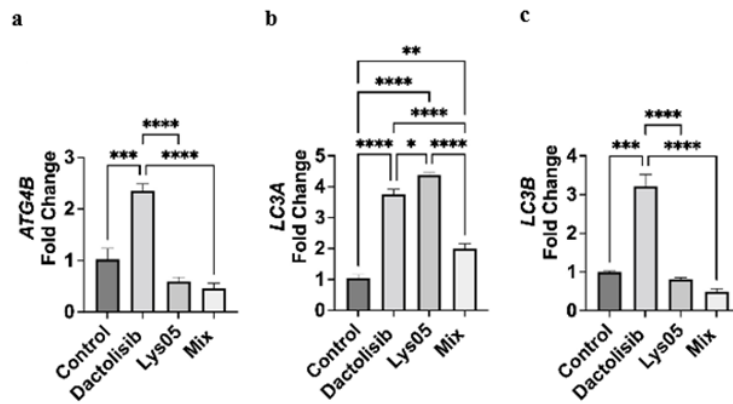
Figure 4. Expression levels of the autophagic markers.
(**a**) *ATG4B,* (**b**) *LC3A and* (**c**) *LC3B* genes in A549 control cells, Dactolisib-treated cells (0.375 μM), Lys05-treated cells (11.8 μM) and mix-treated cells (0.05 μM Dactolisib + 3.19 μM Lys05).

additive. The synergistic effect indicates that the combination is more effective than individual treatments alone.

Treatment of starved A549 cells with Lys05 plus dactolisib with various combination ratios, the IC_{50} value of the 2:1 ratio (2L/1D) (0.05 μM Dactolisib + 3.19 μM Lys05) showed a significant effect below the additive line, indicating a synergistic effect with combination index "CI" 0.4.

Table 1. The combination index "CI" of IC50 values of various combination ratios.

	Ratio		
	(2L/1D)	L/D	(1L/2D)
Combination Index: "CI"	0.4	0.91	1.2

Dactolisib and Lys05 individually and in combination altered the expression of autophagic, proliferative, and apoptotic gene markers

Using quantitative real-time PCR, the gene expression levels of the autophagic markers *ATG4B*, *LC3A*, and *LC3B* were determined. In Dactolisib-treated cells, the levels of *ATG4B, LC3A*, and *LC3B* were found to be elevated compared to control cells. Conversely, in Lys05-treated cells, only *LC3A* showed a significant increase in expression compared to control cells (Fig. 4a).

Interestingly, in the mix-treated cells (combination of Dactolisib and Lys05), while *ATG4B* and *LC3B* were downregulated, *LC3A* exhibited a significant increase in expression compared to control cells (Fig. 4a).

These results indicate that Dactolisib treatment leads to the upregulation of *ATG4B, LC3A*, and *LC3B*, suggestingthe induction of autophagy. In contrast, Lys05 treatment primarily upregulates the expression of *LC3A*. Notably, in the mix-treated cells, the combination of Dactolisib and Lys05 resulted in the downregulation of *ATG4B* and *LC3B*, but a significant increase in *LC3A* expression compared to control cells.

These findings suggest that the combination treatment may have a distinct effect on autophagic markers compared to individual treatments alone.

The expression levels of *CASP3* and *KI67* were examined in different treatment groups compared to control cells

Firstly, it was observed that *CASP3*, a marker of apoptosis, showed a considerable elevation in mix-treated cells compared to control cells (Fig. 5a). This suggests that the combination treatment of Dactolisib and Lys05 induced a higher level of *CASP3* expression, indicating an increased apoptotic response. Additionally, *CASP3* was also found to be upregulated in cells treated with Dactolisib alone and Lys05 alone, indicating that both individual treatments could induce apoptosis to some extent.

Secondly, the expression *KI67*, a marker of cellular proliferation, was significantly downregulated in cells treated with Dactolisib, Lys05, and the mix of Dactolisib and Lys05 (Fig. 5b).

This suggests that Dactolisib, Lys05, and the combination treatments inhibited cellular proliferation, as evidenced by the reduced expression of *KI67*.

Overall, these results indicate that the mix-treated cells had a notable elevation in *CASP3* expression, indicating an enhanced apoptotic response compared to control cells. Additionally, both Dactolisib, Lys05 and the mix of Dactolisib and Lys05 resulted in the downregulation of *KI67*, suggesting inhibition of cellular proliferation.
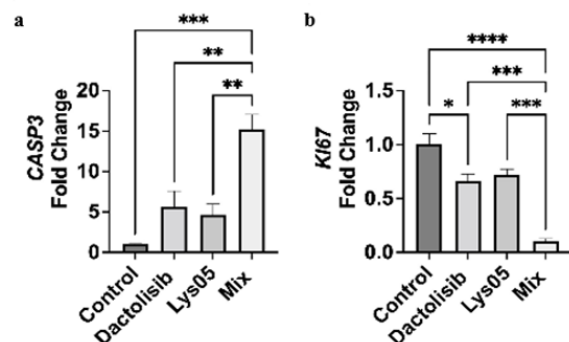
Figure 5. Expression levels of apoptotic and proliferative markers.
(**a**) *CASP3* and (**b**) *KI67* genes in A549 control cells, Dactolisib-treated cells (0.375 μM), Lys05-treated cells (11.8 μM) and mix-treated cells (0.05 μM Dactolisib + 3.19 μM Lys05).
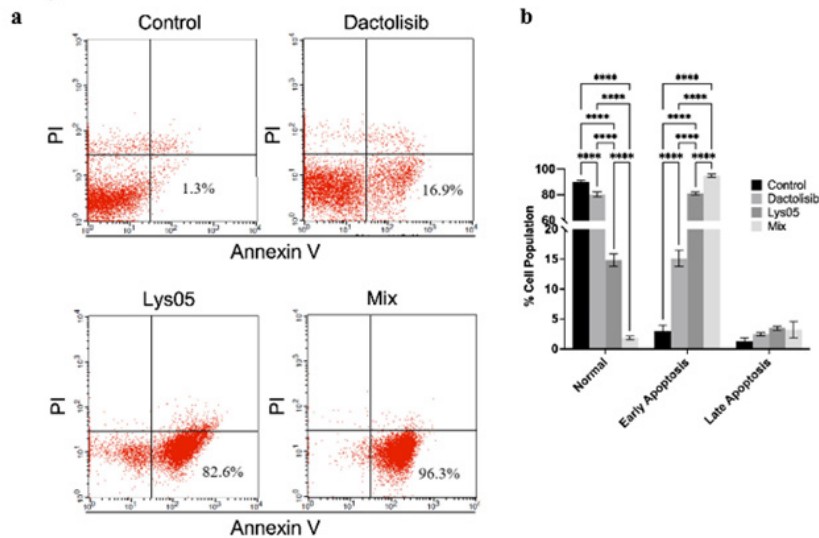
Figure 6. Apoptosis detection through flow cytometry.
(**a**) A549 control cells, Dactolisib-treated cells (0.375 μM), Lys05-treated cells (11.8 μM) and mix-treated cells (0.05 μM Dactolisib + 3.19 μM Lys05). Apoptosis was analyzed through double staining with Propidium iodide and Annexin V-FITC. The lower left quadrant represents control cells, the lower right quadrant represents cells in early apoptosis, the upper right quadrant represents cells in late apoptosis and the upper left quadrant represent cells in necrosis. (**b**) Quantitative analysis of cell population in early, late apoptosis, and necrosis in control A549 cells, Dactolisib-treated cells, Lys05-treated cells and mix-treated cells.

Dactolisib/Lys05 combination enhances killing in A549 cells

Flow cytometry was employed to evaluate the induction of apoptosis in starved A549 cells following treatment with Dactolisib, Lys05, or a combination of both. The percentage of cells undergoing early apoptosis was determined for each treatment group.

The results showed that Dactolisib treatment led to an early apoptosis percentage of 16.9%. Lys05 treatment exhibited a significantly higher early apoptosis percentage of 82.6%. Notably, when the two drugs were combined (mix), the early apoptosis percentage dramatically increased to 96.3%. In comparison, the control group of untreated A549 cells had an early apoptosis percentage of 1.3% (Fig. 6).

These findings indicate that both Dactolisib and Lys05 treatments can induce apoptosis in starved A549 cells. However, the combination of Dactolisib and Lys05

(mix) resulted in a much higher early apoptosis percentage compared to either treatment alone or the control group. This suggests a synergistic effect between Dactolisib and Lys05 in promoting apoptosis in A549 cells.

Dactolisib and Lys05 individually and in combination alter the expression of autophagic protein markers on A549 cells

The expression levels of P62/SQSTM1, LC3A, and LC3B were assessed in different treatment groups compared to control cells.

Firstly, it was found that the expression of P62/SQSTM1, a protein involved in autophagy, was significantly increased in Lys05-treated cells and mix-treated cells compared to control cells (Fig. 7a). This suggests that both Lys05 treatment and the combination treatment led to an upregulation of P62/SQSTM1 expression, indicating a potential disruption in the autophagic process.
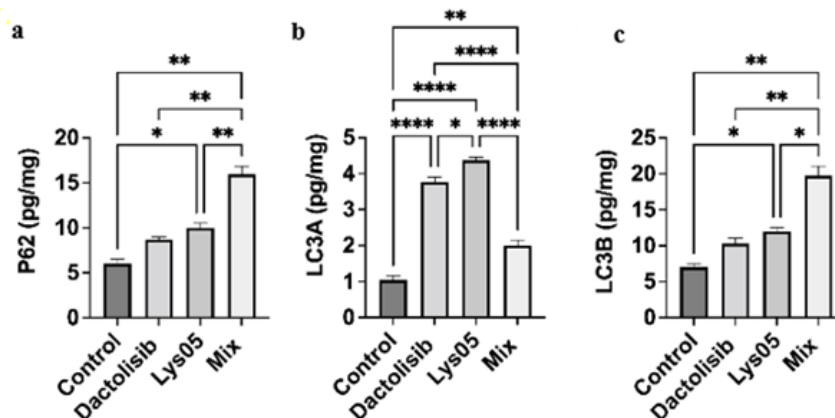
Figure 7. ELISA assay of autophagic protein markers.
(**a**) P62 protein, (**b**) LC3A protein and (**c**) LC3B protein on control A549 cells, Dactolisib-treated cells (0.375 μM), Lys05-treated cells (11.8 μM) and mix-treated cells (0.05 μM Dactolisib + 3.19 μM Lys05)

Secondly, the levels of LC3A, an autophagy-related protein, were significantly higher in mix-treated cells compared to control cells (Fig. 7b). This indicates that the combination treatment resulted in an increased expression of LC3A, suggesting the induction of autophagy. Similarly, LC3B showed a significant increase in expression in Lys05-treated cells (Fig. 7c). Interestingly, the same pattern was observed in cells treated with the combination of both drugs, indicating a consistent effect.

Overall, these results demonstrate that the Lys05 treatment and the combination treatment (mix) led to an upregulation of P62/SQSTM1 expression. Furthermore, the combination treatment resulted in higher levels of LC3A expression compared to control cells, while Lys05 treatment specifically increased LC3B expression. These findings suggest a potential modulation of autophagy-related proteins by the treatments, indicating a complex interplay between autophagy and the therapeutic effects of Lys05 and the combination treatment.

In the experiment, a semi-quantitative analysis of LC3B expression was conducted using Image J software. Figure 8 illustrates the results of this analysis, showing the upregulation of LC3B in Lys05-treated cells and mix-treated cells compared to the untreated control A549 cells.

The upregulation of LC3B in Lys05-treated cells and mix-treated cells suggests an increase in autophagy activity. LC3B is a well-known marker for autophagosomes, which are structures involved in the autophagy process. The upregulation of LC3B indicates an accumulation of autophagosomes, suggesting an enhancement of the autophagic response in the treated cells.

The semi-quantitative analysis performed using Image J software allows for the quantification and comparison of LC3B expression levels between different treatment groups. The results clearly demonstrate the higher expression of LC3B in Lys05-treated cells and mix-treated cells, highlighting the impact of these treatments on autophagy induction.

DISCUSSION:

Indeed, the PI3K/mTOR signaling pathway plays a crucial role in various aspects of cancer development
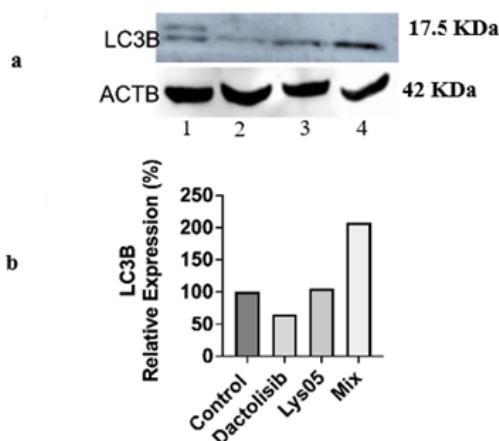
Figure 8. Western blot analysis of LC3B expression in A549 cells. After treatment with Dactolisib and Lys05 individually and in combination. (a) Lane 1 represents A549 control cells, lane 2 represents Dactolisib-treated cells (0.375 µM), lane 3 represents Lys05-treated cells (11.8 µM) and lane 4 represents mix-treated cells (0.05 µM Dactolisib + 3.19 µM Lys05). (b) Chart represents LC3B expression level.

and progression, including cell proliferation, angiogenesis, invasion, cell survival, and motility. Dysregulation of this pathway has been frequently observed in many types of cancer, making it an attractive target for developing novel anticancer agents (Samuels et al., 2004).

Targeting the PI3K/mTOR pathway has shown promise as a therapeutic approach in cancer treatment. By inhibiting specific components or key signaling molecules within this pathway, it is possible to disrupt the aberrant signaling cascade and potentially halt or slow down cancer progression (Herrera et al., 2011).

Several studies have investigated the development of novel anticancer agents that target the PI3K/mTOR pathway. These agents aim to selectively inhibit the activity of specific enzymes or molecules within the pathway, thereby modulating its downstream effects on cell proliferation, angiogenesis, invasion, and survival (Herrera et al., 2011).

Previously, it has been revealed that inhibition of the PI3K/mTOR pathway induces autophagy as a mechanism of cell death or drug resistance (Fujiwara et al., 2007; Yang et al., 2011). Therefore, the inhibition of autophagy in addition to targeting the PI3K/Akt/mTOR pathway may enhance cancer cell death.

In our study, we examined the cytotoxic effect of the two drugs on MCF-7 and A549 cells. The IC50 values for each cell line were determined and presented in Fig. 1 for MCF-7 cells and Figure 2 for A549 cells. The results revealed that A549 cells exhibited greater sensitivity to the two drugs compared to MCF-7 cells.

Additionally, we investigated the effect of combining Lys05 and Dactolisib on starved A549 cells using different ratios. Among the combination ratios tested, the 2:1 ratio (2 parts Lys05 to 1 part Dactolisib) demonstrated a significant effect below the additive line, indicating a synergistic effect. The combination index (CI) value of 0.4, as shown in Figure 3, further supports the synergistic interaction between the two drugs.

Furthermore, we investigated the gene expression levels of autophagic markers, namely ATG4B, LC3A, and LC3B, using quantitative real-time PCR. ATG4B is an autophagic cysteine protease responsible for cleaving the pre-protein ATG8, specifically LC3, resulting in the formation of the non-lipidated soluble form (LC3A). The cleaved LC3A can then interact with phosphatidylethanolamine to form the lipidated form (LC3B), which is anchored to the autophagic membrane (Xia et al., 2022).

Our gene expression analysis revealed significant upregulation of ATG4B, LC3A, and LC3B in Dactolisib-treated cells compared to the control cells, indicating autophagic induction (p values = 0.0009 for ATG4B, 0.0001 for LC3A, and 0.0003 for LC3B) (Fig. 4a, 4b, and 4c, respectively). Similarly, in Lys05-treated cells, we observed a significant upregulation of LC3A (p = 0.0001) (Fig. 4a) as a compensatory mechanism in response to Lys05-induced autophagic inhibition. However, ATG4B and LC3B showed obvious downregulation, suggesting autophagosome inhibition.

In mix-treated cells, we found that LC3A was significantly upregulated compared to the control cells (p = 0.0032) (Fig. 4a). However, both ATG4B and LC3B were downregulated, likely due to the combined effect of the two drugs. These findings indicate that the combination of Dactolisib and Lys05 exerted a significant effect on A549 cells, modulating autophagic processes through differential regulation of autophagic markers.

Furthermore, we examined the gene expression levels of a proliferative marker, KI67, and an apoptotic marker, CASP3. CASP3 is an executioner caspase involved

in apoptosis that coordinates the degradation of cellular structures (Ma *et al.*, 2021). KI67 is an antigen associated with nuclear proliferation and is expressed during the growth and synthesis phases of the cell cycle (G1, S, G2, and M), but not during the resting phase (G0) (Gerdes *et al.*, 1991).

Our results demonstrated that Ki-67 was significantly downregulated in Dactolisib-treated cells and mix-treated cells compared to control cells (p=0.0244 and 0.0001, respectively) (Fig. 5b). This suggests that the treatment with Dactolisib and the combination of the two drugs resulted in a suppression of proliferation in A549 cells.

In contrast, CASP3 was upregulated in Dactolisib-treated cells and Lys05-treated cells. Notably, it was significantly upregulated in mix-treated cells compared to control cells (p=0.0007) (Fig. 5a). These findings indicate that the combination of Dactolisib and Lys05 had a significant impact on promoting apoptosis in A549 cells.

Taken together, our results demonstrate the significant effects of the drug combination on both the proliferative and apoptotic levels in A549 cells, as evidenced by the downregulation of the proliferative marker KI67 and the upregulation of the apoptotic marker CASP3.

It is well-established that the evasion of regulated modes of cell death is a hallmark of cancer (Sharma *et al.*, 2019). In our study, we further supported our findings regarding apoptotic and proliferative levels using flow cytometry analysis. Annexin V/PI staining of A549 cells treated with dactolisib, Lys05, and the combination (Mix) revealed percentages of early apoptosis at 16.9%, 82.6%, and 96.3%, respectively (Fig. 6). In comparison, the control untreated A549 cells exhibited an early apoptosis rate of 1.3%. These results clearly demonstrate that our combination treatment has a significant effect on both proliferation and apoptosis in A549 cells.

Furthermore, to support our gene expression findings, we performed additional analyses using ELISA for p62/SQSTM1 and LC3s (MAP1-LC3A and B), and Western blot for LC3B. P62/SQSTM1 acts as a receptor for cargo destined to be degraded by autophagy, including ubiquitinated protein aggregates targeted for clearance. The p62 protein can bind to both ubiquitin and LC3, facilitating the targeting of cargo to autophagosomes for degradation (Berkamp *et al.*, 2021). LC3s (MAP1-LC3A and B) are structural proteins found in autophagosomal membranes and are widely used as biomarkers of autophagy (Koukourakis *et al.*, 2015).

Our results revealed that p62/SQSTM1 was significantly upregulated in both Lys05- and mix-treated cells (p=0.0305 and 0.0011, respectively) compared to the control (Fig. 7a). This upregulation indicates autophagic inhibition. Additionally, LC3A was significantly upregulated in mix-treated cells (p=0.0044) (Fig. 7b). On the other hand, LC3B was significantly upregulated in Lys05-treated cells (p=0.0482) (Fig. 7c) due to its accumulation resulting from autophagic inhibition. Similarly, mix-treated cells exhibited the same pattern of upregulation in LC3B due to the combined effect of the two drugs (p=0.0017). The semi-quantified Western blot analysis of LC3B aligned with the ELISA results (Fig. 8). These findings strongly support the efficacy of our drug combination.

Considering the comprehensive findings from our study, it is evident that the combination of kinase inhibitor and autophagy inhibitor led to increased cell killing, as demonstrated by enhanced annexin V/PI staining, upregulation of the apoptotic gene marker CASP3, and downregulation of the proliferative gene marker KI67. This combination exhibited a synergistic effect on A549 cells compared to each drug used alone. Therefore, we can confidently conclude that the kinase inhibitor/autophagy inhibitor combination provides greater therapeutic benefits for A549 cells compared to monotherapy with kinase inhibitors alone. This synergistic effect has also been observed in other studies involving glioma (Cerniglia *et al.*, 2012) and malignant peripheral nerve sheath tumors (Ghadimi *et al.*, 2012), further supporting the significance of our findings.

Declarations

Conflict of interest. We declare that there is no conflict of interest regarding this article. None of the authors have any financial employment, consultancies, honoraria, stock ownership or options, expert testimony, or royalties related to this manuscript. Furthermore, we affirm that this work has not been published elsewhere, is not currently being considered for publication elsewhere, and all authors have given their consent for the submission of this manuscript.

REFERENCES

Adjei AA, Mauer A, Bruzek L, Marks RS, Hillman S, Geyer S, Hanson LJ, Wright JJ, Erlichman C, Kaufmann SH, Vokes EE (2003) Phase II study of the farnesyl transferase inhibitor R115777 in patients with advanced non-small-cell lung cancer. *J Clin Oncol* **21**: 1760–1766. https://doi.org/10.1200/JCO.2003.09.075

Barta JA, Powell CA, Wisnivesky JP (2019) Global epidemiology of lung cancer. *Ann Glob Health* **85**. https://doi.org/10.5334/AOGH.2419

Berkamp S, Mostafavi S, Sachse C (2021) Structure and function of p62/SQSTM1 in the emerging framework of phase separation. *FEBS J* **288**: 6927–6941. https://doi.org/10.1111/FEBS.15672

Bradford MM (1976) A rapid and sensitive method for the quantitation of microgram quantities of protein utilizing the principle of protein-dye binding. *Anal Biochem* **72**: 248–254. https://doi.org/10.1016/0003-2697(76)90527-3

Cerniglia GJ, Karar J, Tyagi S, Christofidou-Solomidou M, Rengan R, Koumenis C, Maity A (2012) Inhibition of autophagy as a strategy to augment radiosensitization by the dual phosphatidylinositol 3-kinase/mammalian target of rapamycin inhibitor NVP-BEZ235. *Mol Pharmacol* **82**: 1230–1240. https://doi.org/10.1124/mol.112.080408

Chen K, Shang Z, Dai AL, Dai PL (2020) Novel PI3K/Akt/mTOR pathway inhibitors plus radiotherapy: Strategy for non-small cell lung cancer with mutant RAS gene. *Life Sci* **255**. https://doi.org/10.1016/j.lfs.2020.117816

Chou TC (2006) Theoretical basis, experimental design, and computerized simulation of synergism and antagonism in drug combination studies. *Pharmacol Rev* **58**: 621–681. https://doi.org/10.1124/pr.58.3.10

El Osta B, Behera M, Kim S, Berry LD, Sica G, Pillai RN, Owonikoko TK, Kris MG, Johnson BE, Kwiatkowski DJ, Sholl LM, Aisner DL, Bunn PA, Khuri FR, Ramalingam SS (2019) Characteristics and outcomes of patients with metastatic kras-mutant lung adenocarcinomas: the lung cancer mutation consortium experience. *J Thorac Oncol* **14**: 876–889. https://doi.org/10.1016/J.JTHO.2019.01.020

Eng CH, Wang Z, Tkach D, Toral-Barza L, Ugwonali S, Liu S, Fitzgerald SL, George E, Frias E, Cochran N, De Jesus R, McAllister G, Hoffman GR, Bray K, Lemon LA, Lucas J, Fantin VR, Abraham RT, Murphy LO, Nyfeler B (2016) Macroautophagy is dispensable for growth of KRAS mutant tumors and chloroquine efficacy. *Proc Natl Acad Sci U S A* **113**: 182–187. https://doi.org/10.1073/PNAS.1515617113

Fujiwara K, Iwado E, Mills GB, Sawaya R, Kondo S, Kondo Y (2007) Akt inhibitor shows anticancer and radiosensitizing effects in malignant glioma cells by inducing autophagy. *Int J Oncol* **31**: 753–760. https://doi.org/10.3892/IJO.31.4.753

Gerdes J, Li L, Schlueter C, Duchrow M, Wohlenberg C, Gerlach C, Stahmer I, Kloth S, Brandt E, Flad HD (1991) Immunobiochemical and molecular biologic characterization of the cell proliferation-associated nuclear antigen that is defined by monoclonal antibody Ki-67. *Am J Pathol* **138**: 867

Ghadimi MP, Lopez G, Torres KE, Belousov R, Young ED, Liu J, Brewer KJ, Hoffman A, Lusby K, Lazar AJ, Pollock RE, Lev D (2012) Targeting the PI3K/mTOR axis, alone and in combination with autophagy blockade, for the treatment of malignant peripheral nerve sheath tumors. *Mol Cancer Ther*. https://doi.org/10.1158/1535-7163.MCT-12-0015

Ghimessy A, Radeczky P, Laszlo V, Hegedus B, Renyi-Vamos F, Fillinger J, Klepetko W, Lang C, Dome B, Megyesfalvi Z (2020) Current therapy of KRAS-mutant lung cancer. *Cancer Metastasis Rev* **39**: 1159–1177. https://doi.org/10.1007/s10555-020-09903-9

Haider T, Pandey V, Banjare N, Gupta PN, Soni V (2020) Drug resistance in cancer: mechanisms and tackling strategies. *Pharmacol Rep*, **72**: 1125–1151. https://doi.org/10.1007/S43440-020-00138-7

Hanahan D, Weinberg RA (2011) Hallmarks of cancer: the next generation. *Cell* **144**: 646–674. https://doi.org/10.1016/J.CELL.2011.02.013

Herrera VA, Zeindl-Eberhart E, Jung A, Huber RM, Bergner A (2011) The dual PI3K/mTOR inhibitor BEZ235 is effective in lung cancer cell lines. *Anticancer Res* **31**: 849–854

Heymach JV, Johnson DH, Khuri FR, Safran H, Schlabach LL, Yunus F, De Vore RF, De Porre PM, Richards HM, Jia X, Zhang S, Johnson BE (2004) Phase II study of the farnesyl transferase inhibitor R115777 in patients with sensitive relapse small-cell lung cancer. *Ann Oncol* **15**: 1187–1193. https://doi.org/10.1093/ANNONC/MDH315

Huang L, Guo Z, Wang F, Fu L (2021) KRAS mutation: from undruggable to druggable in cancer. *Signal Transduct Target Ther* **6**: 1–20. https://doi.org/10.1038/s41392-021-00780-4

Koukourakis MI, Kalamida D, Giatromanolaki A, Zois CE, Sivridis E, Pouliliou S, Mitrakas A, Gatter KC, Harris AL (2015) Autophagosome proteins LC3A, LC3B, and LC3C have distinct subcellular distribution kinetics and expression in cancer cell lines. *PloS One* **10**. https://doi.org/10.1371/JOURNAL.PONE.0137675

Kumar P, Nagarajan A, Uchil PD (2018) Analysis of cell viability by the MTT Assay. *Cold Spring Harb Protoc* **2018**: 469–471. https://doi.org/10.1101/PDB.PROT095505

Lakshmanan I, Batra SK (2013) Protocol for apoptosis assay by flow cytometry using annexin V staining method. *Bio-Protoc*: e374. http://www.bio-protocol.org/e374

Lee MG, Lee KS, Nam KS (2021) Arctigenin-mediated cell death of SK-BR-3 cells is caused by HER2 inhibition and autophagy-linked apoptosis. *Pharmacol Rep* **73**: 629–641. https://doi.org/10.1007/S43440-021-00223-5

Liang SQ, Bührer ED, Berezowska S, Thomas, Marti M, Xu D, Froment L, Yang H, Hall SRR, Vassella E, Yang, Zhang, Kocher GJ, Amrein MA, Riether, Carsten, Ochsenbein AF, Schmid RA, Peng RW (2019) mTOR mediates a mechanism of resistance to chemotherapy and defines a rational combination strategy to treat KRAS-mutant lung cancer. *Oncogene*. https://doi.org/10.1038/s41388-018-0479-6

Lim SM, Mohamad Hanif EA, Chin SF (2021) Is targeting autophagy mechanism in cancer a good approach? The possible double-edge sword effect. *Cell Biosci* **11**: 1–13. https://doi.org/10.1186/S13578-021-00570-Z

Liu Y, Song A, Wu H, Sun Y, Dai M (2021) Paeonol inhibits apoptosis of vascular smooth muscle cells *via* up-regulation of autophagy by activating class III PI3K/Beclin-1 signaling pathway. *Life Sci* **264**: 118714. https://doi.org/10.1016/J.LFS.2020.118714

Liu ZQ, Mahmood T, Yang PC (2014) Western blot: technique, theory, and troubleshooting. *NAJMS* **6**: 160. https://doi.org/10.4103/1947-2714.128482

Lohinai Z, Klikovits T, Moldvay J, Ostoros G, Raso E, Timar J, Fabian K, Kovalszky I, Kenessey I, Aigner C, Renyi-Vamos F, Klepetko W, Dome B, Hegedus B (2017) KRAS-mutation incidence and prognostic value are metastatic site-specific in lung adenocarcinoma: poor prognosis in patients with KRAS mutation and bone metastasis. *Sci Rep* **7**. https://doi.org/10.1038/SREP39721

Luo J, Ostrem J, Pellini B, Imbody D, Stern Y, Solanki HS, Haura EB, Villaruz LC (2022) Overcoming KRAS-mutant lung cancer. *ASCO* **42**: 1–11. https://doi.org/10.1200/EDBK_360354

Ma X, Zhang J, Wang Z (2021) Real-time monitoring of active caspase 3 during AFB1 induced apoptosis based on SERS-fluorescent dual mode signals. *SAA* **263**. https://doi.org/10.1016/J.SAA.2021.120195

Rao X, Huang X, Zhou Z, Lin X (2013) An improvement of the 2^(-delta delta CT) method for quantitative real-time polymerase chain reaction data analysis. *Biostat Bioinforma Biomath* **3**: 71-85.

Rio DC, Ares M, Hannon GJ, Nilsen TW (2010) Purification of RNA using TRIzol (TRI Reagent) *Cold Spring Harb Protoc* **5**. https://doi.org/10.1101/PDB.PROT5439

Rizzo P, Osipo C, Foreman K, Golde T, Osborne B, Miele L (2008) Rational targeting of Notch signaling in cancer. *Oncogene* **27**: 5124–5131

Samuels Y, Wang Z, Bardelli A, Silliman N, Ptak J, Szabo S, Yan H, Gazdar A, Powell SM, Riggins GJ, Willson JKV, Markowitz S, Kinzler KW, Vogelstein B, Velculescu VE (2004) High frequency of mutations of the PIK3CA gene in human cancers. *Science* **304**: 554. https://doi.org/10.1126/SCIENCE.1096502/SUPPL_FILE/SAMUELS.SOM.PDF

Sever R, Brugge JS (2015) Signal transduction in cancer. *CSH Perspect Med* **5**. https://doi.org/10.1101/CSHPERSPECT.A006098

Sharma A, Boise LH, Shanmugam M (2019) Cancer metabolism and the evasion of apoptotic cell death. *Cancers* **11**. https://doi.org/10.3390/CANCERS11081144

Sun X, Li K, Zhao R, Sun Y, Xu J, Peng ZY, Song RD, Ren H, Tang SC (2021) Lung cancer pathogenesis and poor response to therapy were dependent on driver oncogenic mutations. *Life Sci* **265**. https://doi.org/10.1016/J.LFS.2020.118797

Wang X, Liu J, Xie Z, Rao J, Xu G, Huang K, Li W, Yin Z (2019) Chlorogenic acid inhibits proliferation and induces apoptosis in A498 human kidney cancer cells *via* inactivating PI3K/Akt/mTOR signalling pathway. *J Pharm Pharmacol* **71**: 1100–1109. https://doi.org/10.1111/JPHP.13095

White E (2012) Deconvoluting the context-dependent role for autophagy in cancer. *Nat Rev Cancer*. https://doi.org/10.1038/nrc3262

White E, DiPaola RS (2009) The double-edged sword of autophagy modulation in cancer. *Clin Cancer Res* **15**: 5308–5316. https://doi.org/10.1158/1078-0432.CCR-07-5023

Xia F, Fu Y, Xie H, Chen Y, Fang D, Zhang W, Liu P, Li M (2022) Suppression of ATG4B by copper inhibits autophagy and involves in Mallory body formation. *Redox Biol* **52**: 102284. https://doi.org/10.1016/J.REDOX.2022.102284

Yang S, Xiao X, Meng X, Leslie KK (2011) A mechanism for synergy with combined mTOR and PI3 kinase inhibitors. *PLOS One* **6**: e26343. https://doi.org/10.1371/JOURNAL.PONE.0026343

Yu X, Li Y, Jiang G, Fang J, You Z, Shao G, Zhang Z, Jiao A, Peng X (2021) FGF21 promotes non-small cell lung cancer progression by SIRT1/PI3K/AKT signaling. *Life Sci* **269**: 118875. https://doi.org/10.1016/J.LFS.2020.118875

Zhao R, Chen M, Jiang Z, Zhao F, Xi B, Zhang X, Fu H, Zhou K (2015) Platycodin-D induced autophagy in non-small cell lung cancer cells *via* PI3K/Akt/mTOR and MAPK signaling pathways. *J Cancer* **6**: 623–631. https://doi.org/10.7150/JCA.11291

Zou Z, Tao T, Li H, Zhu X (2020) MTOR signaling pathway and mTOR inhibitors in cancer: Progress and challenges. *Cell Biosci* **10**. https://doi.org/10.1186/S13578-020-00396-1